Shape-memory properties of crosslinked biobased polyurethanes

Tamara Calvo-Correas[1], Nagore Gabilondo[1], Ana Alonso-Varona[2], Teodoro Palomares[2], M. Angeles Corcuera[1], Arantxa Eceiza[1]*

[1] *Group 'Materials + Technologies', Department of Chemical and Environmental Engineering, Polytechnic School, University of the Basque Country, Pza Europa 1, Donostia-San Sebastian, 20018, Spain*

[2] *Department of Cellular Biology and Histology, Faculty of Medicine and Odontology, University of the Basque Country UPV/EHU, B Sarriena, s/n 48940, Leioa-Bizkaia, Spain*

tamara.calvo@ehu.eus, nagore.gabilondo@ehu.eus, ana.alonsovarona@ehu.eus, teodoro.palomares@ehu.eus, marian.corcuera@ehu.eus

**corresponding author: arantxa.eceiza@ehu.eus*

ABSTRACT

Biobased crosslinked polyurethanes were synthesized and characterized as shape-memory polymers. Both the macrodiol and the diisocyanate were derived from renewable sources; the first one from castor oil, and the second one from L-lysine amino acid. The influence of component molar ratios, crosslink density and maximum elongation on the shape-memory properties was analyzed. The thermal analysis showed that polyurethanes were microphase separated. Though the study of the shape-memory properties, it was seen that shape-memory was influenced by crosslink density. A higher crosslink density led to a greater shape recovery, since crosslinks are the responsible for memorizing the shape of the material. With the increase of maximum elongation, both shape fixity and recovery decreased due to higher amount of crosslink net points were broken. Moreover, the synthesized polyurethanes showed its potential to be used in biomedical applications, according to the preliminary in vitro cytotoxicity assays.

Key words: crosslinked polyurethane, biobased diisocyanate, shape-memory

INTRODUCTION

The development of shape-memory polymers (SMPs) has drawn increasing attention among smart materials in the last years, due to SMPs can find broad applications in different sectors ranging from the aerospace to the biomedical [1–7]. These kind of smart materials are able to remember their original shape after being deformed and recover it as a response to an external stimulus, being heat the most common [8,9]. In general, the physical (crystalline segregated domains or entanglements) or chemical crosslink (covalent bonding) of thermoresponsive polymers are the responsible for memorizing the shape [10,11]. While the so-called switching phase serves as a molecular switch and enables the fixation of the temporary shape [12,13] showing a transition temperature (T_{trans}), which can either be a glass transition (T_g) or a melting temperature (T_m). During the shape-memory test the material is heated and deformed in a temperature above the T_{trans}, named as switching temperature (T_s), and it is subsequently quench at a temperature below T_{trans} in order to fix the shape. Once the sample is reheated above T_{trans} its original shape is restored [14]. Shape-memory properties are dependent on the morphology, the degree of microphase separation and the conditions at which the tests were carried out [13,15]. In addition, in chemically crosslinked SMPs the crosslink density also influences on shape-memory properties, due to it determines the relative motion of segments and net points, and hence the capability of the polymer to recover to its original shape after being deformed [8]. Moreover, in materials with a broad thermal transition, the so-called

temperature-memory effect (TME) takes place, when the temperature at which the deformation is applied is within the range of the thermal transition [16–20].

Segmented polyurethanes are one of the most noteworthy SMPs [9,21–24], due to their versatility, which enables the synthesis of materials with different properties just by manipulating their composition. Segmented polyurethanes are block copolymers composed by two blocks, one formed by a macrodiol (polyether or polyester diol), and the other composed by a diisocyanate and a low molecular weight chain extender or crosslinker [25,26]. The incompatibility between both segments leads to microphase separation which depends on block lengths, hydrogen bonding and crystallization extent [27,28].

Furthermore, because of economic, environmental and social concerns the interest the synthesis of shape-memory polyurethanes based on components derived from renewable sources is gaining attention. In most of the works, only the polyol is biobased and the diisocyanate used is based on fossil sources [29–31]. Nevertheless, in a recently published work [32] we successfully synthesized biobased thermoresponsive linear thermoplastic polyurethanes, using a macrodiol derived from castor oil, a L-lysine amino acid based diisocyanate and a diol type chain extender derived from corn sugar. Since it was seen that covalently crosslinked polyurethanes show better thermal, thermomechanical and shape-memory properties than linear polyurethanes [33,34], in this work chemically crosslinked polyurethanes were synthesized, using the same macrodiol and diisocyanate employed previously [32]. As crosslinker the 1,1,1-tris-(hydroxymethyl)propane (TMP) with primary hydroxyl groups was employed.

Differential scanning calorimetry (DSC) and dynamic mechanical analysis (DMA) were used in order to establish the transition temperatures of the thermally-responsive polyurethanes. Furthermore, in order to analyze physicochemical properties of the material Fourier transform infrared spectroscopy (FTIR) was used. The mechanical properties of the synthesized polyurethanes were analyzed by performing tensile and Shore D hardness tests. In the same way, the study of thermally-activated shape-memory properties was carried out by means of thermo-mechanical cyclic test. Finally, preliminary evaluation of the *in vitro* cytotoxicity and surface properties were also estimated.

EXPERIMENTAL

Materials

Poly(butylene sebacate)diol derived from castor oil, with a number-average molecular weight of 3505 g mol^{-1} and a hydroxyl index of 32.01 determined by titration with ASTM D 4274-88 Test Method A [35] was used as macrodiol. Ethyl ester L-lysine diisocyanate (226 g mol^{-1}) and 1,1,1-tris-(hydroxymethyl)propane (134.17 g mol^{-1}) crosslinker were supplied by CHEMOS GmbH and Fluka, respectively. The macrodiol was dried under vacuum for 6 h at 80 °C prior to use. The chemical structures of the macrodiol, diisocyanate and crosslinker are shown in Figure 1.

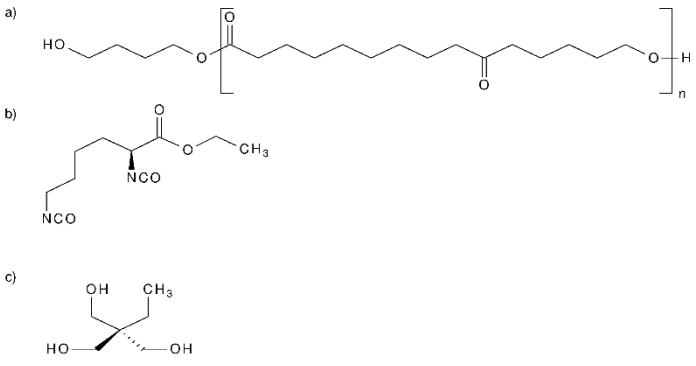

Figure 1. Structure of the different materials used in the synthesis: poly(butylene sebacate)diol (a), ethyl ester L-lysine diisocyanate (b) and 1,1,1-tris-(hydroxymethyl)propane (c).

Synthesis of the polyurethanes

Polyurethanes were synthesized by two step bulk polymerization procedure. The reaction was carried out in a 250 mL five-necked round-bottom flask equipped with a mechanical stirrer and dry nitrogen inlet. Firstly, dried polyol and diisocyanate were placed in the flask and heated in a thermo-regulated silicon bath at 100 °C for 5 h. Then, the crosslinker was added to the prepolymer at 100 °C and the mixture was rapidly stirred for 10-15 min. Finally the resulting viscous liquid was quickly poured between two Teflon® coated metal plates separated by 1.5 mm and pressed at 100 °C under 50 bar for 10 h. The NCO to OH groups molar ratio of all polyurethanes was kept constant at 1.01. Designation, macrodiol/LDI/TMP molar ratios and LDI/TMP segment content of the polyurethanes are shown in Table 1. As a reference pure LDI/TMP segment (PUTMP 100) was also synthesized.

Table 1. Designation, molar ratio and LDI/TMP content of the polyurethanes.

Sample designation	Molar ratio Macrodiol/LDI/TMP	LDI/TMP (wt%)[a]
PUTMP20	1/3/2	20
PUTMP30	1/5/4	30
PUTMP40	1/ 8/7	40
PUTMP100	0/1/1	100

[a] LDI/TMP content calculated as weight percentage of LDI and TMP with respect to total polyurethane weight

Characterization techniques

Fourier transform infrared spectroscopy

Polyurethane characteristic functional groups and hydrogen-bonding were analyzed by FTIR, on a Nicolet Nexus spectrometer with a MKII Golden Gate accessory with diamond crystal at a nominal incident angle of 45° and a ZnSe lens. The spectra were obtained after 32 scans in a range from 4000 to 650 cm^{-1} with a resolution of 4 cm^{-1} in transmittance mode.

FTIR is widely employed in order to estimate the degree of phase separation (DPS) [36,37]. According to Pretsch et al. [37], the carbonyl hydrogen bonding index (R) was determined by analyzing the intensities of the carbonyl stretching vibration of free and hydrogen-bonded groups, which were deconvoluted using the Gaussian curve-fitting method in OriginPro 8.6 software, from equation 1. Afterwards, the degree of phase separation was calculated through equation 2

$$R = A_{bonded} / A_{free} = (C_{bonded}\ \varepsilon_{bonded}) / (C_{free}\ \varepsilon_{free}) \quad (1)$$

$$DPS = C_{bonded} / (C_{bonded}+C_{free}) = R / (R+1) \quad (2)$$

where A_{bonded} and A_{free} are the intensities of the characteristic absorbances, C_{bonded} and C_{free} the concentrations and ε_{free} and ε_{bonded} the extinction coefficients of free and hydrogen-bonded carbonyl bands. According to Seymour et al. [38] the ratio $\varepsilon_{bonded}/\varepsilon_{free}$ could be considered as 1, so that the carbonyl hydrogen-bonding index is directly equal to the ratio of C_{bonded}/C_{free}.

Differential scanning calorimetry

Thermal properties were investigated by means of DSC using a Mettler Toledo DSC822e equipment, provided with a robotic arm and an electric intracooler as a refrigeration unit. Samples with a weight between 5 and 10 mg were sealed in aluminum pans and heated from -75 °C to 150 °C at a scanning rate of 20 °C min^{-1}, using N_2 as a purge gas (20 mL min^{-1}). The crystallization process was also followed by cooling the samples from 150 °C to -75 °C at scanning rate of 10 °C min^{-1}. A second heating run were also performed, but as the results did not provide any extra information, they are not reported here. The inflexion point of the heat capacity change observed was chosen to evaluate the glass transition temperature, T_g. Melting temperature (T_m) was settled as the maximum of endothermic peak taking the area under the peak as melting enthalpy (ΔH_m). Crystallization temperature (T_c) was taken as the minimum of the exothermic peak observed in the cooling scan and the crystallization enthalpy (ΔH_c) as the peak area. Taking into account the melting or crystallization enthalpy values and based on equations (3) and (4), the relative crystallinity (χ_c) (crystallinity of the phase to the crystallinity of the neat phase) were measured for each of the polyurethanes synthesized in the heating ($\chi_{c\ heating}$) and cooling ($\chi_{c\ cooling}$) scans [39]:

$$\chi_c = \Delta H_e/\Delta H_t \quad (3)$$

$$\Delta H_t = \Delta H_p * \omega \quad (4)$$

where ΔH_e is the experimental melting or crystallization enthalpy value and ΔH_t is the theoretical value calculated by equation (2), where ΔH_p is the melting or crystallization enthalpy value of the corresponding neat phase and ω is the weight enthalpy fraction of that phase.

Dynamic mechanical analysis

The dynamic mechanical behavior of the polyurethanes was analyzed by DMA in tensile mode on an Eplexor 100 N analyzer from Gabo, using an initial strain of 0.10%. The temperature was varied from -100 to 150 °C at a scanning rate of 2 °C min^{-1} and at a fixed operation frequency of 10 Hz. Samples were cut in strips of 22 mm in length, 5 mm in width and 1.5 mm in thickness.

Mechanical properties and shape-memory behavior

Mechanical testing was carried out at room temperature using a Universal Testing Machine (MTS Insight 10) with a load cell of 10 kN and pneumatic grips. Samples were cut into dog-bone shape according to ASTM D1708-93 standard. Tests were performed with a crosshead rate of 50 mm min^{-1}. Elastic modulus (E), tensile strength at break (σ) and percentage elongation at break (ε) were averaged from at least five test specimen data.

Shore D hardness measurements were performed at room temperature with a MD-202 DuroTECH digital hardness testing device following ASTM D2240 standard. Results were averaged from a least five values measured in several zones of the sample.

The shape-memory properties of the polyurethanes were studied in the strain-controlled mode using the MTS Insight 10 equipment. Samples were cut in strips of 22 mm in length, 5 mm in width and 1.5 mm in thickness and heated at the switching temperature for 10 min. Thereafter, samples were stretched up to different elongations at a rate of 5 mm min^{-1}, using sandpaper pasted into pneumatic grips in order to avoid slipping. Once the maximum elongation was reached, the sample was cooled down below T_{trans} to fix the temporary shape and the applied stress was removed. The permanent shape was recovered upon heating the sample up to switching temperature for 10 min. Five thermo-mechanical cyclic tensile tests were consecutively performed.

Thermally activated shape-memory behavior was quantified following the commonly used parameters. The shape fixity (R_f) and shape recovery (R_r) ratios can be calculated using equations 5 and 6, respectively.

$$R_f(N) = \varepsilon_u(N)/\varepsilon_m(N) \quad (5)$$

$$R_r(N) = (\varepsilon_m(N) - \varepsilon_p(N)) / (\varepsilon_m(N) - \varepsilon_p(N-1)) \quad (6)$$

where ε_m is the maximum strain in the tensile test, ε_U is the residual strain after unloading to below T_{trans}, ε_P is the residual strain after the shape recovery and N is the number of cycles.

Cytotoxicity

To assess *in vitro* cell response, short-term cytotoxicity evaluation was carried out using L-929 murine fibroblasts cells, following ISO 10993 standard part 5 guidelines [40]. To prepare extracts of test materials, samples with an area of 6 cm^2 were rinsed with Mili-Q water, sterilized with 100% ethylene oxide gas, and allowed at least 7 days to degas. Sterilized film samples were incubated separately in standard cell culture medium (Dulbecco's modified Eagle's medium [Sigma Chemicals Co, USA] plus 10% fetal calf serum [Gibco] and supplemented with antibiotic-antimycotic solution [Sigma]) at 37 °C for 24 h to obtain the extracted culture media. In addition, L-929 murine fibroblasts were firstly seeded and allowed to grow in 96-well microplates at a density of 4×10^3 cells/well in the presence of standard culture medium for 24 h before the experiments. In the cytotoxicity test, cultures were treated for 24, 48 and 72 h with the extracted media. As controls, standard culture media (control) were used, high-density polyethylene (negative control, USP Rockville, USA), and polyvinyl chloride (positive control, Portex, UK).

To evaluate cell viability and proliferation, metabolic activity of viable cells was determined using the colorimetric assay MTT (Cell Proliferation Kit I MTT, Roche). This test is based on reduction of 3-(4,5-dimethyltriazol-2yl)-2,5 diphenyltetrazolium bromide on formazan in the mitochondria of living cells. The cell number per well was proportional to the amount of formazan crystals and was determined by measuring the absorbance at 540 nm using a microplate reader (ELISA). Viability (%) was calculated from equation 7:

$$\text{Viability (\%)} = ([A]_{test} / [A]_{control}) *100 \quad (7)$$

where $[A]_{test}$ is the absorbance of the sample cells and $[A]_{control}$ is the absorbance of the negative control cells, in this case high-density polyethylene. All assays were conducted in triplicate and average values and their standard deviations were estimated.

Water contact angle

The surface properties of synthesized polyurethanes were evaluated measuring the water contact angle (WCA) in Dataphysics OCA20 equipment. Five measurements of each sample were carried out with a deionised water drop method (2 μL) at 26 °C. The surface energy between the surface of the material and water was calculated using Neumann's Equation of State (8), which is based on the equilibrium of forces at the edge of a resting drop, as proposed by Young.

$$\gamma_{PU} = 1/4 \ \gamma_{H_2O} (1+\cos\beta)^2 \quad (8)$$

where γ_{PU} is the surface energy of the biopolyurethane, γ_{H_2O} is the water surface energy and β is the angle between water drop and biopolyurethane surface.

RESULTS AND DISCUSSION

The characteristic bonds of the polyurethanes were analyzed by means of FTIR. In Figure 2a the infrared spectra of the polyurethanes as well as pure macrodiol and neat LDI spectra are shown. Polyurethanes do not show the band associated with N=C=O group stretching vibration at 2270 cm^{-1}, meaning that all the isocyanate groups have reacted during the polymerization. Furthermore, all of them show a broad band centered at 3350 cm^{-1}, ascribed to the N-H stretching vibration of urethane groups [41]. In the same way, at 1528 cm^{-1} a band associated to C-N stretching vibration combined to N-H out-of-plane bending can be seen [25]. Both bands become more intense as isocyanate content increases due to a higher content of urethane groups. As can be observed in the inset, where the carbonyl group stretching region is shown, the macrodiol and the LDI present a band at 1728 and 1738 cm^{-1} respectively, associated to carbonyl stretching in ester groups [32]. Regarding the synthesized polyurethanes, all of them show a band at 1728 cm^{-1}, encompassing the carbonyl groups of the macrodiol and the LDI. Moreover, this band shows a shoulder around 1698 cm^{-1} [42] attributed to the carbonyl of urethanes groups. Furthermore, as can be observe in Figure 2b, where the peak deconvolution of baseline corrected C=O stretching bands of the synthesized polyurethanes is shown, the intensity of the peak related with hydrogen-bonded carbonyl group (II) increases with the increase of LDI/TMP content. This fact could be attributed to a higher amount of urethane groups per unit volume. The DPS was estimate from the Gaussian peak intensities. PUTMP20, PUTMP30 and PUTMP40 polyurethanes show a DPS of 0.60, 0.59 and 0.64, respectively. As can be seen phase separation slightly increases with the increases of LDI/TMP, suggesting that the mixing of LDI/TMP rich domain into macrodiol rich domain is hindered due to LDI/TMP domains are larger.

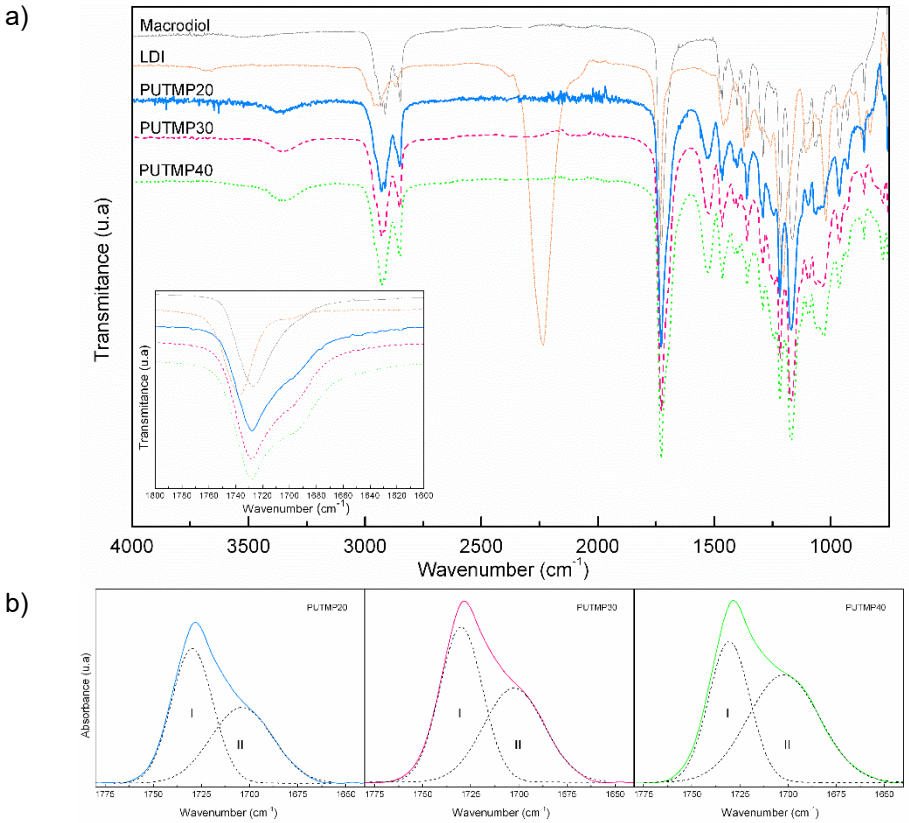

Figure 2. FTIR spectra of the synthesized polyurethanes, macrodiol and LDI. (a) Inset: carbonyl group stretching region and peak deconvolution (dot lines) of baseline corrected C=O stretching bands of the synthesized polyurethanes, C=O free stretching (I) and C=O hydrogen-bonded stretching (II) bands (b).

The study of the thermal transitions of the material is essential in order to determine the test conditions, and also to understand the shape-memory behavior. Figure 3 shows the heating DSC thermograms of the synthesized polyurethanes with different LDI/TMP content, together with the thermograms of pure macrodiol and neat LDI/TMP. The thermal transitions are listed in Table 2.

Table 2. Thermal transitions values of macrodiol and the synthesized polyurethanes.

Sample	T_{g1} (ºC)	T_m (ºC)	ΔHm (J g^{-1})	T_{g2} (ºC)	ΔH_c (J g^{-1})	T_c (ºC)	χ_c heating	χ_c cooling	ν_e (mol m^{-3})
Macrodiol	-52.0	70.0	142.0	-	-93.1	46.3	1	1	-
PUTMP20	-40.0	65.0	77.8	13.6	-51.0	32.1	0.7	0.7	201
PUTMP30	-48.1	52.8	54.2	19.1	-36.5	20.9	0.5	0.6	241
PUTMP40	-46.6	52.2	52.7	22.6	-24.9	18.4	0.6	0.5	313
PUTMP100	-	-	-	59.3	-	-	-	-	-

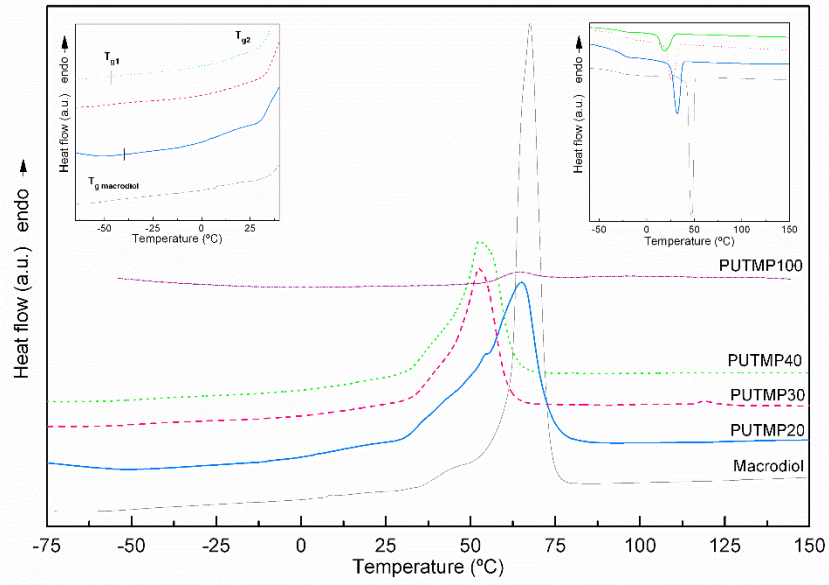

Figure 3. Heating DSC thermograms of the synthesized polyurethanes, macrodiol and neat LDI/TMP. Left inset: magnification of the low temperature region. Right inset: cooling DSC thermograms.

The semicrystalline macrodiol shows a T_g at -52 ºC and an endothermic peak associated to crystals melting centered at 70 ºC. However, the amorphous LDI/TMP shows a T_g at 59 ºC. Regarding the synthesized polyurethanes, all of them show several thermal transitions related to those observed for the macrodiol and the neat LDI/TMP. At low temperature in the interval of -60 ºC and -40 ºC, polyurethanes show a glass transition (T_{g1}) (inset on the left), which becomes closer to the T_g of the neat macrodiol as LDI/TMP content increases, suggesting a microphase separated microstructure, despite a small amount of covalently bonded LDI/TMP could be mixed within the macrodiol rich domain. Moreover, all the polyurethanes show a broad endothermic peak associated to the melting temperature of ordered domains mainly formed by the macrodiol. As LDI/TMP content increases the melting enthalpy and temperature decrease, due to the lower amount of crystallizable macrodiol fraction and also due to the chemically crosslinked LDI/TMP fractions, which inhibits the mobility of chains, hindering the crystallization [2,43]. As can be seen in Table 2, the relative crystallinity values decreased with the increase of LDI/TMP content. Moreover, the cooling scans (inset on the right) show a similar behavior, where as LDI/TMP content increases crystallization temperature and enthalpy also decrease.

The relative crystallinity values are similar to those determined in the heating scan. All the polyurethanes show a second glass transition (T_{g2}) associated to the domain mainly formed by LDI/TMP between the T_{g1} and T_m of the macrodiol rich domain, which increases as LDI/TMP content increases, becoming closer to the T_g of neat LDI/TMP, due to the formation of more crosslinked structure. Since all polyurethanes show two separated glass transition temperatures, becoming closer to the T_g of neat components as LDI/TMP content increases, the polyurethanes presents a phase separated microstructure [44], which corroborates the results observed by FTIR. The dynamical mechanical behavior of the polyurethanes was analyzed in order to follow the changes in the viscoelastic properties and also to determine the crosslink density. The temperature dependence of the storage modulus (E') and loss factor (tanδ) for the synthesized polyurethanes is shown in Figure 4.

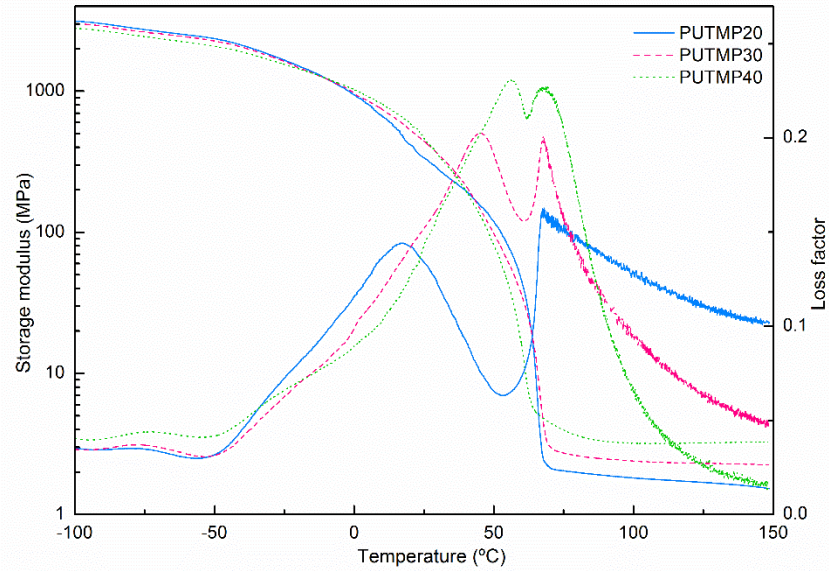

Figure 4. Storage modulus and loss factor of the synthesized polyurethanes.

As can be seen, as macrodiol content increases, the storage modulus values in the glassy state increase, due to the crystallinity of this domain. Therefore it is expected that PUTMP20 sample would show a better shape fixation, due to the higher the modulus in the glassy state is, the greater the shape fixity is [2]. Above -50 ºC, a slight decrease in E' can be observed, as well as, a shoulder in tanδ, which is related with the T_g of the macrodiol rich domain (T_{g1}) as previously observed by DSC. At higher temperatures a broad E' decrease can be seen associated with the glass transition temperature of the LDI/TMP rich domain and melting temperature of the macrodiol rich domain. After the decrease of E', the material reaches the rubbery plateau, where the storage modulus value increases with the increase of LDI/TMP rich domain content, according to a more crosslinked structure which provides significant structural reinforcement and a higher elastic recovery force at high temperature [2,35]. Regarding tanδ curve a maximum can be observed, which is related with the glass transition of the LDI/TMP rich domain (T_{g2}), which increases as LDI/TMP content increases in accordance to DSC results. Moreover, the crosslink density (ν_e) [45] values were calculated following the equation 9

$$\nu_e = E'/(3RT) \quad (9)$$

where E' is the storage modulus in the rubbery region (T_g + 75 ºC), R is the universal constant of gases (8.314 J mol^{-1} K^{-1}) and T is the temperature in Kelvin. The relative crosslink densities of the polyurethanes are gathered in Table 2. As can be observed, crosslink density increases with the increase of LDI/TMP, and therefore the amount of crosslink agent, meaning that the chain segments are more closely restricted by net points which inhibit the mobility. Since in thermoset polymers the shape recovery is given through covalently bonded net points [8,10,34], it is foreseen that polymers with higher LDI/TMP content would show higher shape recovery.

Taking into account the results obtained by both DSC and DMA measurements, 40 ºC was chosen as switching temperature in order to assess shape-memory properties. This temperature is within the interval of T_{g2} of the LDI/TMP rich domain and T_m of the macrodiol rich domain.

In order to determine the strain at which the samples were stretch up in the thermo-mechanical tensile tests, mechanical properties were analyzed. Figure 5 shows the strain-stress curves and the values derived from them together hardness Shore D values are displayed in Table 3.

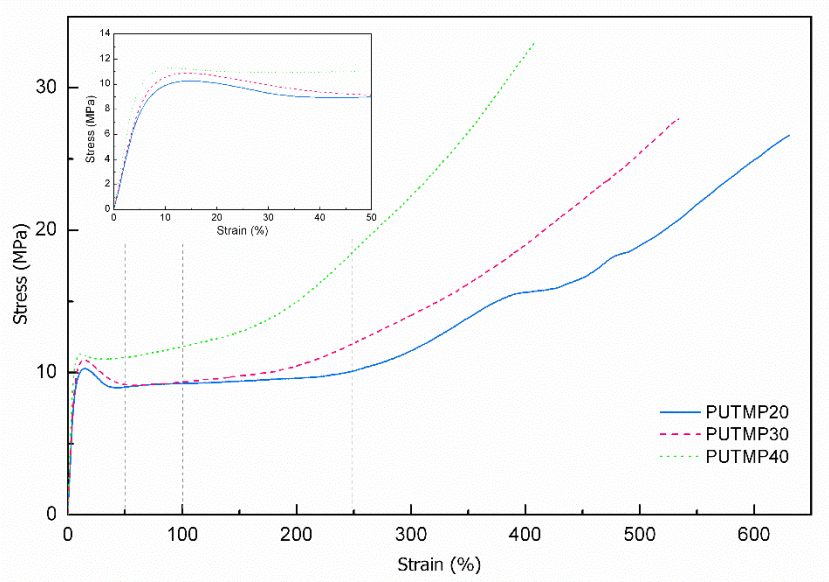

Figure 5. Stress-strain curves of the synthesized polyurethanes. Inset: magnification from 0 to 50 % of elongation.

Table 3. Mechanical properties of the synthesized polyurethanes systems.

Sample	E (MPa)	σ (MPa)	ε (%)	Shore D
PUTMP20	169.1 ± 8.5	27.5 ± 1.2	629.0 ± 11.2	54.0 ± 0.4
PUTMP30	179.4 ± 6.6	29.1 ± 1.0	559.9 ± 30.3	57.0 ± 0.5
PUTMP40	245.0 ± 3.1	32.0 ± 1.6	398.6 ± 15.3	58.6 ± 0.5

As LDI/TMP content increases the material withstands higher elastic modulus and stresses, while elongation decreases. This fact is due to the three-dimensional structure formed through covalent bonds, where net points are the responsible for carrying the load, avoiding chains slipping. As LDI/TMP content increases the crosslink density increases and hence the distance between net points become smaller, resulting in an increase in the elastic modulus and a decrease in elongation [8]. Moreover, the more crosslinked structure enhances the hardness of the material. In the strain-stress curves it can be seen, that the material shows different behaviors. Once the yield point is exceeded, it can be observed a plateau, where stress does not significantly change with strain. At elongations higher than 150%, stress increases with the

increase of strain, showing a quasi-elastic behavior. Taking these different behaviors into account, the thermo-mechanical tensile tests were performed at three different elongations, 50%, 100% and 250%, which are associated to the intervals with the observed behaviors.

As far as thermally-activated shape-memory effects of the synthesized polyurethanes is concerned, the stress-strain curves for the successive thermo-mechanical cycles at elongations of 50%, 100% and 250% are illustrated in Supporting information Figure 1. Moreover, R_f and R_r values are summarized in Table 4.

Table 4. R_f and R_r values calculated for each thermo-mechanical cycle at different maximum stretching elongations for the synthesized polyurethanes.

ε_m (%)	Cycle	PUTMP20		PUTMP30		PUTMP40	
		R_f (%)	R_r (%)	R_f (%)	R_r (%)	R_f (%)	R_r (%)
50	1	96.9	81.7	93.9	89.5	88.9	93.1
	2	94.7	98.9	92.0	99.9	92.4	98.7
	3	93.8	99.1	91.5	99.9	90.6	99.0
	4	94.5	99.8	90.1	99.6	90.1	99.0
	5	93.2	99.8	90.1	99.6	89.7	99.5
100	1	88.6	78.1	87.7	83.8	86.4	85.0
	2	91.6	97.1	89.8	93.3	89.1	97.7
	3	91.0	97.5	93.5	99.6	92.3	98.4
	4	93.7	99.3	89.5	99.2	90.6	99.3
	5	92.3	99.5	90.3	99.6	88.6	100.0
250	1	80.0	72.4	77.1	75.8	72.0	84.7
	2	80.9	90.4	83.1	95.8	79.3	94.8
	3	83.3	99.7	84.3	97.0	74.3	98.3

Regarding the results obtained in the first cycle at maximum elongation of 50%, R_f values of the polyurethanes range from 97% to 89%, and R_r values from 82% to 93%. As can be observed in Table 4, as LDI/TMP content increases R_f decreases due to a higher crosslink density. Since shape-memory effect is an entropic phenomenon [13,33], when crosslink density increases chains are more closely restricted providing a greater steric hindrance, which inhibits chains conformations to adopt the lowest entropy state and hence decreases the shape fixation. Regarding shape recovery, as LDI/TMP content increases R_r increases according to a greater physical and chemical crosslink density. Polymers with a higher crosslink density have a greater elastic strain energy stored, which provides them a higher driving force for subsequent thermally induced shape recovery, due to the driving force responsible for shape recovery is in fact the residual stress introduced in the sample during the stretching process [8,46]. Furthermore, as all samples were stretched over the yield point in the first cycle, plastic deformation take place, resulting in the break of some chemical and physical bonds, which allows the shifting of the chains. Therefore, in the first cycle, the R_r values will not reach 100%, and the original shape cannot be completely restored [2,9]. Moreover, regarding the so-called temperature-memory effect observed in a previous work [32] since the overlapped area is similar for all the compositions (12.0, 10.6 and 10.0 J g^{-1} for PUTMP20, PUTMP30 and PUTMP40 respectively) the contribution to the rubbery state would be alike for all systems.

In order to understand how the increase of the maximum elongation influences on shape-memory properties, the thermo-mechanical cyclic tensile tests were also carried out at maximum elongation of 100% and 250%. The shape-memory behavior in the first cycle is

similar to the one observed at 50%, as LDI/TMP content increases R_f decreases while R_r increases. However, at higher maximum elongations the material withstands a greater plastic deformation and hence a higher amount of physical and chemical bonds are broken and therefore lower R_r values were measured. In the same way, with the increase of the maximum elongation the R_f decreases. When the maximum elongation is 250%, the stress that the polyurethanes withstand increases from one cycle to another (Supporting information Figure 1 down). This behavior is known as “cyclic hardening” and is due to a relaxation of the material in the stretched state which results in a higher orientation and crystallization of the chains, as observed in Figure 5. In this way, the material is more resistant against the strain from cycle to cycle [12,47,48].

Since T_{trans} of the synthesized polyurethanes is bellow or close to room temperature, they should be stored bellow its T_{trans}. Therefore, in order to verify if the material is able to keep the fixed shape over time, once the last thermo-mechanical cyclic tensile test was performed, the sample was stretched up again to each maximum elongation and quenched in order to fix the shape and kept at 4 °C in a refrigerator. After 2 months it was seen that all samples still maintained the fixed shape. Subsequently, the samples were heat up to T_s and they were able to restore their shape obtaining R_r values similar to previous ones.

As shape-memory polymers could be used for biomedical applications, short-term cytotoxicity assays for the synthesized polyurethanes were carried out, which give information about the cell response after incubation in the extracted media from sterilized material with respect to the cells cultured in standard culture media (negative control) [29,49]. The viability analysis performed in the first 24 h shows that the material has a non-toxic behavior, since cell viability value is around 90% of the value of negative control, which was higher than the acceptance limit of 70%, as established by ISO 10993-12 standard (Figure 6a).

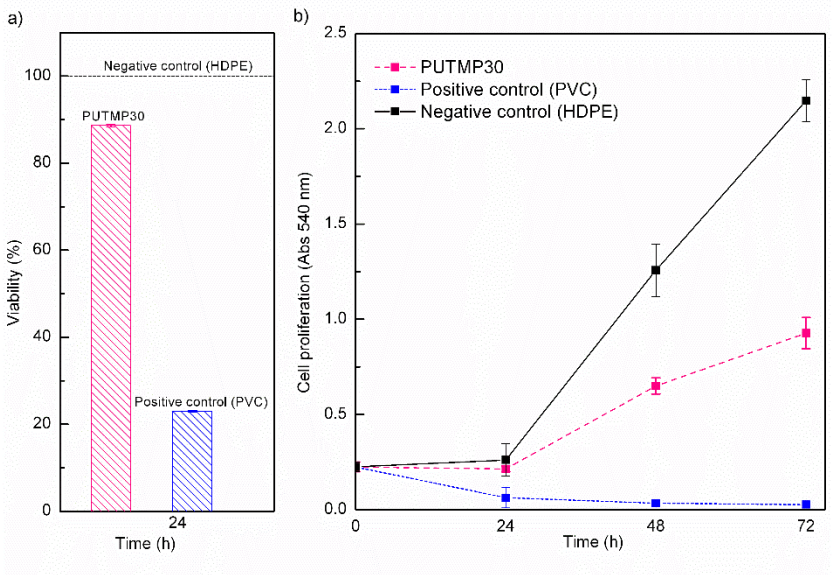

Figure 6. Viability of L-929 murine fibroblast cells in extracted media at 24 (a) and absorbance at 540 nm versus incubation time of a positive control (PVC), negative control (HDPE) and PUTMP 30 polyurethane (b).

In addition, we determine the cell proliferation activity during 72 h in the presence of the extracted media. As can be seen in Figure 6b, cell proliferation was as expected when cells were cultured in negative and positive control media, showing a sharp growth in the case of HDPE (negative control) and a drastic reduction in cell number in the case of PVC (positive control), which is derived from its known cytotoxic effect. Similarly to the negative control, cells

cultured in PUTMP30-extracted media also shows a marked growth from 24 to 72 h demonstrating that this material has the potential to be exploited in biomedicine.

Since shape-memory properties could be deteriorated by the hydrophilic character, wettability and surface energy of the material, the contact angle of the synthesized polyurethanes was analyzed. Contact angle analysis provides information of the surface hydrophobicity or hydrophilicity, and of the molecular mobility at the air-water-solid interface [50,51]. In the Table 5 the contact angle and surface energy values of the synthesized polyurethanes are gathered. Usually, as urethanes group density increases, the hydrophobicity decreases, showing lower water contact angle values as previously observed [32]. However, in the synthesized crosslinked polyurethanes the opposite behavior was seen which can be attributed to a higher crosslink density [52].

Table 5. Contact angle and surface energy values of synthesized polyurethanes.

	Contact angle (°)	Surface energy (mN m^{-1})
PUTMP20	72.78 ± 0.72	30.6
PUTMP30	79.66 ± 0.22	25.3
PUTMP40	83.55 ± 0.52	22.5

CONCLUSIONS

A diisocyanate from L-lysine amino acid was used for the synthesis of thermally-responsive crosslinked biobased polyurethanes, as well as, a macrodiol derived from castor oil. he synthesized polyurethanes were phased separated, with a crosslinked microdomain formed by LDI/TMP with a glass transition temperature close to room temperature and a crystallizable microdomain formed by the macrodiol. Shape-memory properties were analyzed at 40 ºC, bellow of the macrodiol microdomain melting temperature. It was observed that shape-memory properties varied with crosslink density, allowing obtaining biobased polyurethanes with tailored shape-memory properties. As crosslink density increased R_f decreased, according to a higher steric hindrance which inhibited chain conformations to adopt the lowest entropy state. Moreover, R_r increased with the increased of the crosslink density, showing that the net points of the structure contribute also to memorize the shape. It was seen that the highest R_r and R_f values were obtained when the maximum elongation was closer to the yield point. The *in vitro* preliminary biocompatibility assay shows that PUTMP30 exhibited no cytotoxicity, thus the polyurethanes synthesized in this work can be considered as potential smart materials for biomedical applications.

ACKNOWLEDGEMENTS

Financial support from the Basque Government (IT-776-13) and from the Spanish Ministry of Economy and Competitiveness (MINECO) (MAT2013-43076-R) is gratefully acknowledged. We also wish to acknowledge the “Macrobehavior-Mesostructure-Nanotechnology” SGIker unit from the University of the Basque Country, for their technical support. T.C-C. thanks the University of the Basque Country for Ph.D. grant (PIF/UPV/12/200).

REFERENCES

[1] J. Leng, X. Lan, Y. Liu, S. Du. Shape-memory polymers and their composites: Stimulus methods and applications. Prog. Mater. Sci. 56 (2011) 1077–1135. doi:10.1016/j.pmatsci.2011.03.001.

[2] D. Ratna, J. Karger-Kocsis. Recent advances in shape memory polymers and

composites: A review. J. Mater. Sci. 43 (2008) 254–269. doi:10.1007/s10853-007-2176-7.

[3] P.T. Mather, X. Luo, I.A. Rousseau. Shape Memory Polymer Research. Annu. Rev. Mater. Res. 39 (2009) 445–471. doi:10.1146/annurev-matsci-082908-145419.

[4] N. Fritzsche, T. Pretsch. Programming of Temperature-Memory Onsets in a Semicrystalline Polyurethane Elastomer. Macromolecules 47 (2014) 5952–5959. doi:10.1021/Ma501171p.

[5] T. Pretsch, M. Ecker, M. Schildhauer, M. Maskos. Switchable information carriers based on shape memory polymer. J. Mater. Chem. 22 (2012) 7757. doi:10.1039/c2jm16204k.

[6] P. Singhal, W. Small, E. Cosgriff-Hernandez, D.J. Maitland, T.S. Wilson. Low density biodegradable shape memory polyurethane foams for embolic biomedical applications. Acta Biomater. 10 (2014) 67–76. doi:10.1016/j.actbio.2013.09.027.

[7] S. Imai, K. Sakurai. An actuator of two-way behavior by using two kinds of shape memory polymers with different T_{gS}, Precis. Eng. 37 (2013) 572–579. doi:10.1016/j.precisioneng.2013.01.002.

[8] X.L. Wu, S.F. Kang, X.J. Xu, F. Xiao, X.L. Ge. Effect of the crosslinking density and programming temperature on the shape fixity and shape recovery in epoxy-anhydride shape-memory polymers. J. Appl. Polym. Sci. 131 (2014) doi:10.1002/app.40559.

[9] A. Saralegi, E. Johan Foster, C. Weder, A. Eceiza, M.A. Corcuera, Thermoplastic shape-memory polyurethanes based on natural oils, Smart Mater. Struct. 23 (2014) 025033(9pp) doi:10.1088/0964-1726/23/2/025033.

[10] C.P. Buckley, C. Prisacariu, A. Caraculacu. Novel triol-crosslinked polyurethanes and their thermorheological characterization as shape-memory materials. Polymer 48 (2007) 1388–1396. doi:10.1016/j.polymer.2006.12.051.

[11] C.M. Yakacki, R. Shandas, D. Safranski, A.M. Ortega, K. Sassaman, K. Gall. Strong, tailored, biocompatible shape-memory polymer networks. Adv. Funct. Mater. 18 (2008) 2428–2435. doi:10.1002/adfm.200701049.

[12] A. Lendlein, S. Kelch. Shape-Memory Polymers. Angew. Chem. Int. Ed. 41 (2002) 2034–2057.

[13] J.L. Hu, F.L. Ji, Y.W. Wong. Dependency of the shape memory properties of a polyurethane upon thermomechanical cyclic conditions. Polym. Int. 54 (2005) 600–605. doi:10.1002/pi.1745.

[14] H.M. Jeong, J.H. Song, K.W. Chi, I.K. And, K.T. Kim. Shape memory effect of poly(methylene-1,3-cyclopentane) and its copolymer with polyethylene. Polym. Int. 51 (2002) 275–280. doi:10.1002/pi.823.

[15] M. Behl, A. Lendlein. Shape-memory polymers. Mater. Today 10 (2007) 20–28. doi:10.1016/S1369-7021(07)70047-0.

[16] K. Kratz, U. Voigt, A. Lendlein. Temperature-memory effect of copolyesterurethanes and their application potential in minimally invasive medical technologies. Adv. Funct. Mater. 22 (2012) 3057–3065. doi:10.1002/adfm.201200211.

[17] K. Yu, H.J. Qi. Temperature memory effect in amorphous shape memory polymers. Soft Matter 10 (2014) 9423–9432. doi:10.1039/C4SM01816H.

[18] N. Mirtschin, T. Pretsch. Advances semicrystalline polyurethane. RSC Adv. 5 (2015) 46307–46315. doi:10.1039/C5RA05492C.

[19] W.G. Bae, J.H. Choi, K.Y. Suh. Pitch-tunable size reduction patterning with a temperature-memory polymer. Small. 9 (2013) 193–198. doi:10.1002/smll.201201554.

[20] P. Miaudet, A. Derré, M. Maugey, C. Zakri, P.M. Piccione, R. Inoubli, P. Poulin. Shape and temperature memory of nanocomposites with broadened glass transition. Science 318 (2007) 1294–1296. doi:10.1126/science.1145593.

[21] S. Weng, Z. Xia, J. Chen, L. Gong, Shape memory properties of polycaprolactone-based polyurethanes prepared by reactive extrusion, J. Appl. Polym. Sci. 127 (2013) 748–759. doi:10.1002/app.37768.

[22] M. Bothe, T. Pretsch. Bidirectional actuation of a thermoplastic polyurethane elastomer. J. Mater. Chem. A. 1 (2013) 14491–14497. doi:10.1039/c3ta13414h.

[23] M. Bothe, F. Emmerling, T. Pretsch. Poly(ester urethane) with varying polyester chain length: Polymorphism and shape-memory behavior. Macromol. Chem. Phys. 214 (2013) 2683–2693. doi:10.1002/macp.201300464.

[24] C. Azra, C.J.G. Plummer, J.A.E. Månson. Isothermal recovery rates in shape memory polyurethanes. Smart Mater. Struct. 20 (2011) 082002 (10pp). doi:10.1088/0964-1726/20/8/082002.

[25] M.A. Corcuera, L. Rueda, B. Fernandez d'Arlas, A. Arbelaiz, C. Marieta, I. Mondragon, A. Eceiza. Microstructure and properties of polyurethanes derived from castor oil. Polym. Degrad. Stab. 95 (2010) 2175–2184. doi:10.1016/j.polymdegradstab.2010.03.001.

[26] L. Rueda-Larraz, B. Fernández-d'Arlas, A. Tercjak, A. Ribes, I. Mondragon, A. Eceiza. Synthesis and microstructure-mechanical property relationships of segmented polyurethanes based on a PCL-PTHF-PCL block copolymer as soft segment. Eur. Polym. J. 45 (2009) 2096–2109. doi:10.1016/j.eurpolymj.2009.03.013.

[27] X. Gu, P.T. Mather. Entanglement-based shape memory polyurethanes: Synthesis and characterization. Polymer 53 (2012) 5924–5934. doi:10.1016/j.polymer.2012.09.056.

[28] W. Wang, Y. Jin, P. Ping, X. Chen, X. Jing, Z. Su. Structure evolution in segmented poly(ester urethane) in shape-memory process. Macromolecules 43 (2010) 2942–2947. doi:10.1021/ma902781e.

[29] A. Saralegi, S.C.M. Fernandes, A. Alonso-Varona, T. Palomares, E.J. Foster, C. Weder, A. Eceiza. Shape-memory bionanocomposites based on chitin nanocrystals and thermoplastic polyurethane with a highly crystalline soft segment. Biomacromolecules 14 (2013) 4475–4482. doi:10.1021/bm401385c.

[30] E. Del Rio, G. Lligadas, J.C. Ronda, M. Galià, M.A.R. Meier, V. Cádiz. Polyurethanes from polyols obtained by ADMET polymerization of a castor oil-based diene: Characterization and shape memory properties. J. Polym. Sci. Part A Polym. Chem. 49 (2011) 518–525. doi:10.1002/pola.24466.

[31] M.A. Corcuera, A. Saralegi, B. Fernandez-d'Arlas, I. Mondragon, A. Eceiza. Shape memory polyurethanes based on polyols derived from renewable resources. Macromol. Symp. 321-322 (2012) 197–201. doi:10.1002/masy.201251135.

[32] T. Calvo-Correas, A. Santamaria-Echart, A. Saralegi, L. Martin, Á. Valea, M.A. Corcuera, A. Eceiza. Thermally-responsive biopolyurethanes from a biobased diisocyanate. Eur. Polym. J. 70 (2015) 173–185. doi:10.1016/j.eurpolymj.2015.07.022.

[33] T. Xie. Recent advances in polymer shape memory. Polymer 52 (2011) 4985–5000. doi:10.1016/j.polymer.2011.08.003.

[34] J. Hu, Z. Yang, L. Yeung, F. Ji, Y. Liu. Crosslinked polyurethanes with shape memory properties. Polym. Int. 54 (2005) 854–859. doi:10.1002/pi.1785.

[35] A. Saralegi, L. Rueda, B. Fernández-d'Arlas, I. Mondragon, A. Eceiza, M.A. Corcuera. Thermoplastic polyurethanes from renewable resources: Effect of soft segment chemical structure and molecular weight on morphology and final properties. Polym. Int. 62 (2013) 106–115. doi:10.1002/pi.4330.

[36] B. Fernández-d'Arlas, L. Rueda, K. de la Caba, I. Mondragon, A. Eceiza, Microdomain composition and properties differences of biodegradable polyurethanes based on MDI and HDI, Polym. Eng. Sci. 48 (2008) 519–529. doi:10.1002/pen.

[37] T. Pretsch, I. Jakob, W. Müller. Hydrolytic degradation and functional stability of a segmented shape memory poly(ester urethane). Polym. Degrad. Stab. 94 (2009) 61–73. doi:10.1016/j.polymdegradstab.2008.10.012.

[38] R.W. Seymour, G.M. Estes, S.L. Cooper. Infrared studies of segmented polyurethan elastomers. I. Hydrogen bonding. Macromolecules 3 (1970) 579–583. doi:10.1021/ma60017a021.

[39] B. Wunderlinch. Thermal analysis of polymeric materials. Springer, Berlin, 2005.

[40] International Organization for Standardization, ISO 10993-5. Biological evaluation of medical devices. Test for in vitro cytotoxicity (2009).

[41] Z. Wang, L. Yu, M. Ding, H. Tan, J. Li, Q. Fu, Preparation and rapid degradation of nontoxic biodegradable polyurethanes based on poly(lactic acid)-poly(ethylene glycol)-poly(lactic acid) and l-lysine diisocyanate. Polym. Chem. 2 (2011) 601–607. doi:10.1039/c0py00235f.

[42] L. Ugarte, B. Fernández-d'Arlas, A. Valea, M.L. González, M.A. Corcuera, A. Eceiza. Morphology-properties relationship in high-renewable content polyurethanes. Polym. Eng. Sci. 54 (2014) 2282–2291. doi:10.1002/pen.23777.

[43] I. Kaur, P. Ray. Broader spectrum: Examples. In: A. Bhattacharya, J.W. Rawlins, P. Ray (Eds.). Polym. Grafting Crosslink. John Wiley & Sons, Inc., Hoboken, NJ, USA, 2008.

[44] A. Lendlein, R. Langer. Biodegradable, elastic shape-memory polymers for potential biomedical ppplications. Science 296 (2002) 1673–1676. doi:10.1126/science.1066102.

[45] L. Song, Q. Ye, X. Ge, A. Misra, J.S. Laurence, C.L. Berrie, P. Spencer. Synthesis and evaluation of novel dental monomer with branched aromatic carboxylic acid group. J. Biomed. Mater. Res. B. Appl. Biomater. 102B (2014) 1473–1484. doi:10.1002/jbm.b.33126.

[46] A. Tcharkhtchi, S. Abdallah-Elhirtsi, K. Ebrahimi, J. Fitoussi, M. Shirinbayan, S. Farzaneh. Some new concepts of shape memory effect of polymers. Polymers 6 (2014) 1144–1163. doi:10.3390/polym6041144.

[47] H. Tobushi, S. Hayashi, S. Kojima. Mechanical properties of shape memory polymer of polyurethane series. JSME Int. J. 35 (1992) 296–302.

[48] B. Fernández-d'Arlas, R. Fernández, J. Runt, A. Eceiza. Polyurethanes containing a crystalline polyol and semiflexible urethane segments. J. Appl. Polym. Sci. 132 (2015) 41281. doi:10.1002/app.41281.

[49] L. De Nardo, S. Bertoldi, A. Cigada, M.C. Tanzi, H.J. Haugen, S. Farè. Preparation and characterization of shape memory polymer scaffolds via solvent casting/particulate leaching. J. Appl. Biomater. Funct. Mater. 10 (2012) 119–126. doi:10.5301/JABFM.2012.9706.

[50] M.A. Corcuera, L. Rueda, A. Saralegi, M.D. Martín, B. Fernández-d'Arlas, I. Mondragon, A. Eceiza. Effect of diisocyanate structure on the properties and microstructure of polyurethanes based on polyols derived from renewable resources. J. Appl. Polym. Sci. 122 (2011) 3677–3685. doi:10.1002/app.

[51] H. Yeganeh, M.M. Lakouraj, S. Jamshidi. Synthesis and characterization of novel biodegradable epoxy-modified polyurethane elastomers. J. Polym. Sci. Part A Polym. Chem. 43 (2005) 2985–2996. doi:10.1002/pola.20789.

[52] S. Oprea. Effect of the long chain extender on the properties of linear and castor oil cross-linked PEG-based polyurethane elastomers. J. Mater. Sci. 46 (2011) 2251–2258. doi:10.1007/s10853-010-5064-5.

Supplementary information

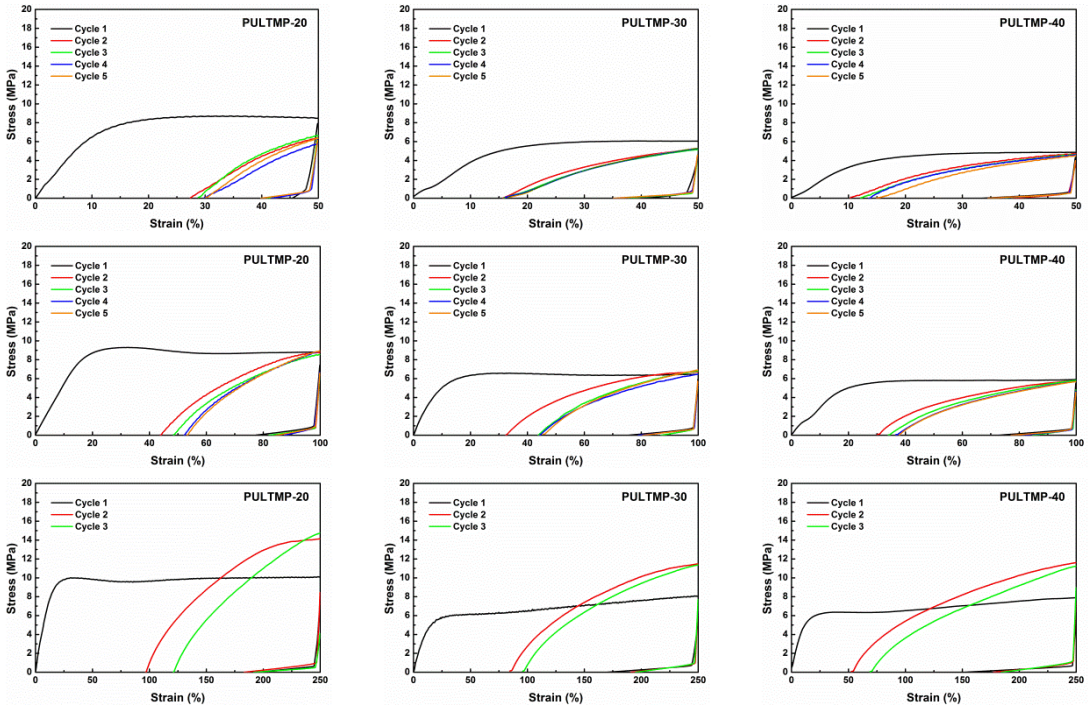

Figure 1. Stress-strain curves of thermo-mechanical cycles performed at 50% (up), 100% (centre) and 250% (down).